Article

Anion-Templated Assembly of Pseudorotaxanes: Importance of Anion Template, Strength of Ion-Pair Thread Association, and Macrocycle Ring Size

Mark R. Sambrook, Paul D. Beer, James A. Wisner, Rowena L. Paul, Andrew R. Cowley, Fridrich Szemes, and Michael G. B. Drew

J. Am. Chem. Soc., **2005**, 127 (7), 2292-2302• DOI: 10.1021/ja046278z • Publication Date (Web): 26 January 2005

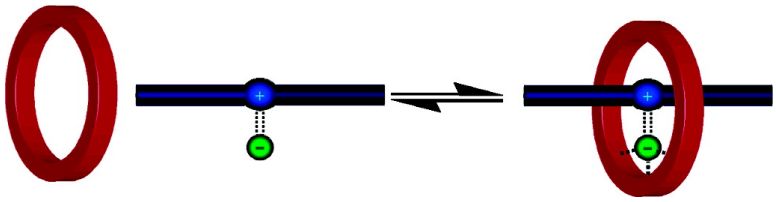

J|A|C|S
ARTICLES
Published on Web 01/26/2005

Anion-Templated Assembly of Pseudorotaxanes: Importance of Anion Template, Strength of Ion-Pair Thread Association, and Macrocycle Ring Size

Mark R. Sambrook,[†] Paul D. Beer,*[,†] James A. Wisner,[†,‡] Rowena L. Paul,[†] Andrew R. Cowley,[†] Fridrich Szemes,[†] and Michael G. B. Drew[§]

Contribution from the Department of Chemistry, Inorganic Chemistry Laboratory, University of Oxford, South Parks Road, Oxford, OX1 3QR, U.K., Department of Chemistry, The University of Western Ontario, Chemistry Building, London, Ontario, N6A 5B7, Canada, and Department of Chemistry, University of Reading, Reading, RG6 6AD, U.K.

Received June 23, 2004; E-mail: paul.beer@chem.ox.ac.uk

Abstract: A wide range of pseudorotaxane assemblies containing positively charged pyridinium, pyridinium nicotinamide, imidazolium, benzimidazolium and guanidinium threading components, and macrocyclic isophthalamide polyether ligands have been prepared using a general anion templation procedure. In noncompetitive solvent media, coupling halide anion recognition by a macrocyclic ligand with ion-pairing between the halide anion and a strongly associated cation provides the driving force for interpenetration. Extensive solution ^{1}H NMR binding studies, thermodynamic investigations, and single-crystal X-ray structure determinations reveal that the nature of the halide anion template, strength of the ion-pairing between the anion template and the cationic threading component, and to a lesser extent favorable second sphere $\pi-\pi$ aromatic stacking interactions between the positively charged threading component and macrocyclic ligand, together with macrocyclic ring size, affect the efficacy of pseudorotaxane formation.

Introduction

Imaginative template methodologies are increasingly being used in the construction of complex supramolecular architectures,[1] ranging from molecular cagelike assemblies and helicates to mechanically interlocked supramolecules, such as rotaxanes, catenanes, and knots.[2] Cationic and neutral species have dominated the templated synthetic strategies reported to date by employing metal−ligand coordination,[3] $\pi-\pi$ stacking interactions,[4] hydrogen bonding,[5] and solvophobic effects[6] to effect assembly between two or more components. The challenge of exploiting anions to direct supramolecular assembly remains largely under-developed, which may be attributed to their diffuse nature, pH dependence, and relative high solvation energy as compared to that of cations.[7] Although various serendipitous discoveries where anions have templated the formation of, in particular, inorganic-based polymetallic cage complexes[8] and circular double helicates[9] have now appeared, strategic anion-templated syntheses and assemblies are rare.[10]

[†] University of Oxford.
[‡] The University of Western Ontario.
[§] University of Reading.

(1) (a) Raymo, F. M.; Stoddart, J. F. *Templated Organic Synthesis*; Wiley: Weinheim, Germany, 2000. (b) *Comprehensive Supramolecular Chemistry*; Sauvage, J.-P., Hosseini, M., Eds.; Elsevier: New York, 1996; Vol. 9. (c) Davis, A. V.; Yeh, R. M.; Raymond, K. N. *Proc. Natl. Acad. Sci. U.S.A.* **2002**, *99* (8), 4793−4796. (d) Furlan, R. L. E.; Otto, S.; Sanders, J. K. M. *Proc. Natl. Acad. Sci. U.S.A.* **2002**, *99* (8), 4801−4804. (e) Krische, M. J.; Lehn, J.-M. *Struct. Bonding* **2000**, *96*, 3−29. (f) Greig, L. M.; Philp, D. *Chem. Soc. Rev.* **2001**, *30*, 287−302. (f) Gale, P. A. *Annu. Rep. Prog. Chem., Sect. B* **2002**, *98*, 581−605. (g) Ward, M. D. *Annu. Rep. Prog. Chem., Sect A* **2002**, *98*, 285−320. (h) Lindsey, J. S. *New. J. Chem.* **1991**, *15* (2−3), 153−180.

(2) (a) Hubin, T. J.; Busch, D. H. *Coord. Chem. Rev.* **2000**, *200−202*, 5−52. (b) Breault, G. A.; Hunter, C. A.; Mayers, P. C. *Tetrahedron* **1999**, *55*, 5265−5293. (c) Panova, I. G.; Topchieva, I. N. *Russ. Chem. Rev.* **2001**, *70* (1), 23−44. (d) Sauvage, J.-P. *Acc. Chem. Res.* **1990**, *23* (10), 319−327.

(3) (a) Dietrich-Buchecker, C. O.; Sauvage. J.-P. *Tetrahedron Lett.* **1983**, *24*, 5095−5098. (b) Dietrich-Buchecker, C. O.; Sauvage, J.-P.; Kern, J.-M. *J. Am. Chem. Soc.* **1984**, *106* (10), 3043−3045. (c) Weck, M.; Mohr, B.; Sauvage, J.-P.; Grubbs, R. H. *J. Org. Chem.* **1999**, *64* (15), 5463−5471. (d) Dietrich-Buchecker, C. O.; Sauvage, J.-P. *Angew. Chem., Int. Ed. Engl.* **1989**, *28*, 189−192. (e) Dietrich-Buchecker, C. O.; Sauvage, J.-P. *Angew. Chem., Int. Ed. Engl.* **1989**, *28*, 189−192. (f) Fujita, M.; Ibukuro, F.; Hagihara, H.; Ogura, K. *Nature* **1994**, *367*, 720−722. (g) Fujita, M.; Ibukuro, F.; Yamaguchi, K.; Ogura, K. *J. Am. Chem. Soc.* **1995**, *117* (14), 4175−4176. (h) Padilla-Tosta, M. E.; Fox, O. D.; Drew, M. G. B.; Beer, P. D. *Angew. Chem., Int. Ed.* **2001**, *40* (22), 4235−4239. (i) Wu, C.; Lecavalier, P. R.; Shen, Y. X.; Gibson, H. W. *Chem. Mater.* **1991**, *3* (4), 569−572.

(4) (a) Ashton, P. R.; Ballardini, R.; Balzani, V.; Bělohradsky, M.; Gandolfi, M. T.; Philp, D.; Prodi, L.; Raymo, F. M.; Reddington, M. V.; Spencer, N.; Stoddart, J. F.; Venturi, M.; Williams, D. J. *J. Am. Chem. Soc.* **1996**, *118* (21), 4931−4951. (b) Stoddart, J. F.; Tseng, H.-R. *Proc. Natl. Acad. Sci. U.S.A.* **2002**, *99* (8), 4797−4800. (c) Raymo, F. M.; Houk, K. N.; Stoddart, J. F. *J. Am. Chem. Soc.* **1998**, *120* (36), 9318−9322. (d) Ashton, P. R.; Baxter, I.; Fyfe, M. C. T.; Raymo, F. M.; Spencer, N.; Stoddart, J. F.; White, A. J. P.; Williams, D. J. *J. Am. Chem. Soc.* **1998**, *120* (10), 2297−2307.

(5) (a) Hunter, C. A. *J. Am. Chem. Soc.* **1992**, *114* (13), 5303−5311. (b) Adams, H.; Carver, F. J.; Hunter, C. A. *Chem. Commun.* **1995**, 809−810. (c) Vögtle, F.; Meier, S.; Hoss, R. *Angew. Chem., Int. Ed. Engl.* **1992**, *31*, 1619−1622. (d) Ottens-Hildebrandt, S.; Nieger, M.; Rissanen, K.; Rouvinen, J.; Meier, S.; Harder, G.; Vögtle, F. J. *Chem. Commun.* **1995**, 777. (e) Johnston, A. G.; Leigh, D. A.; Pritchard, R. J.; Deegan, M. D. *Angew. Chem., Int. Ed. Engl.* **1995**, *34*, 1209−1212.

(6) Anderson, S.; Anderson, H. L. *Angew. Chem., Int. Ed. Engl.* **1996**, *35*, 1956−1958.

(7) Beer, P. D.; Gale P. A. *Angew. Chem., Int. Ed.* **2001**, *40* (3), 486−516.

(8) Fleming, J. S.; Mann, K. L. V.; Carraz, C.-A.; Psillakis, E.; Jeffery, J. C.; McCleverty, J. A.; Ward, M. D. *Angew. Chem., Int. Ed.* **1998**, *37* (9), 1279−1281.

(9) (a) Hasenknopf, B.; Lehn, J.-M.; Kniesel, B. O.; Baum, G.; Fenske, D. *Angew. Chem., Int. Ed. Engl.* **1996**, *35* (16), 1838−1840. (b) Hasenknopf, B.; Leh, J.-M.; Boumediene, N.; Dupont-Gervais, A.; Van Dorsselaer, A.; Kneisel, B.; Fenske, D. *J. Am. Chem. Soc.* **1997**, *119* (45), 10956−10962.

10.1021/ja046278z CCC: $30.25

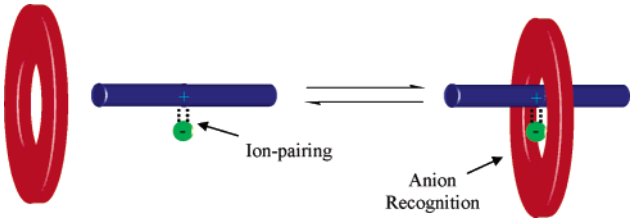

Figure 1. Anion-templated self-assembly of pseudorotaxanes. Recognition of the anion by the macrocycle results in the formation of an interpenetrated structure.

This is especially the case when employing anions in the construction of interpenetrated compounds. Stoddart et al. reported the organizational role a hexafluorophosphate anion can play in the assembly of large [5]- and [6]-pseudorotaxanes from dibenzylammonium threads and polyether macrocycles.[11] Vögtle et. al. have used phenolates, thiophenolates, and sulfonamide anions which when complexed to a cyclic tetralactam and subsequently reacted with a sterically demanding electrophile, affords [2]-rotaxane products in high yields.[12] This elegant anion-templated "snapping" methodology has recently been exploited by Smith in the preparation of a series of ion-pair binding rotaxanes[13] and in a related "stoppering" method of rotaxane formation by Schalley and co-workers.[14]

Herein, we report the use of a rational design procedure to develop a general method of using anions to template the formation of a wide range of pseudorotaxanes, based on the coupling of anion recognition with ion-pairing (Figure 1).[15]

This templation strategy is designed to operate in noncompetitive solvent media where the anion of the ion-pair is strongly associated with the potential cationic threading component and importantly remains coordinatively unsaturated. Subsequent anion recognition by the macrocyclic ligand results in pseudorotaxane formation as the cationic thread strongly associates with the complexed anion within the macrocyclic cavity. The success of this general anion template procedure is illustrated with the halide-directed assembly of a series of novel pseudorotaxanes containing pyridinium, pyridinium nicotinamide, imidazolium, benzimidazolium and guanidinium threading components, and macrocyclic diamide polyether ligands. Solution ^{1}H NMR binding studies and isothermal calorimetry (ITC), together with X-ray crystal structure analyses, demonstrate that the nature of the anion template and the strength of ion-pairing in the threading guest species are both crucial to the thermodynamic stability of pseudorotaxane assembly.[16]

(10) (a) Vilar R. *Angew. Chem., Int. Ed.* **2003**, *42* (13), 1460−1477. (b) Beer, P. D.; Sambrook, M. R. In *Encylopedia of Nanoscience and Nanotechnology*; Marcel Dekker Inc.: New York, in press.
(11) Fyfe, M. C. T.; Glink, P. T.; Menzer, S.; Stoddart, J. F.; White, A. J. P.; Williams, D. J. *Angew. Chem., Int. Ed. Engl.* **1997**, *36* (19), 2068−2070.
(12) (a) Seel, C.; Vögtle, F. *Chem.—Eur. J.* **2000**, *6* (1), 21−24. (b) Reuter, C.; Wienand, W.; Hubner, G. M.; Seel, C.; Vögtle, F. *Chem.—Eur. J.* **1999**, *5* (9), 2692−2697. (c) Hubner, G. M.; Gläser, J.; Seel, C.; Vögtle, F. *Angew. Chem., Int. Ed.* **1999**, *38* (3), 383−386.
(13) (a) Mahoney, J. M.; Shukla, R.; Marshall, R. A.; Beatty, A. M.; Zajicek, J.; Smith, B. D. *J. Org. Chem.* **2002**, *67* (5), 1757−1767. (b) Deetz, M. J.; Shukla, R.; Smith, B. D. *Tetrahedron* **2002**, *58*, 799−805. (c) Shukla, R.; Deetz, M. J.; Smith, B. D. *Chem. Commun.* **2000**, 2397−2398.
(14) Ghosh, P.; Mermagen, O.; Schalley, C. A. *Chem. Commun.* **2002**, 2628−2629.
(15) Jones, J. W.; Gibson, H. W. *J. Am. Chem. Soc.* **2003**, *125* (23), 7001−7004.
(16) Part of this work has been published as preliminary communications: (a) Wisner, J. A.; Beer, P. D.; Drew, M. G. B. *Angew. Chem., Int. Ed.* **2001**, *40* (19), 3606−3609. (b) Wisner, J. A.; Beer, P. D.; Berry, N. G.; Tomapatanaget, B. *Proc. Natl. Acad. Sci. U.S.A.* **2002**, *99* (8), 4983−4986.

Results and Discussion

Thread and Macrocycle Ligand Design for Anion-Templated Pseudorotaxane Formation. When the strategic design features for integrating anionic guest species into a pseudorotaxane superstructure are taken into account (see Figure 1), the anion template is required to simultaneously coordinate two components in an orthogonal fashion. Crabtree and co-workers have shown that simple isophthalamide molecules, such as **1a**, are receptors for anions in chloroform.[17] In particular, they bind chloride, bromide, and iodide anions exclusively in a 1:1 stoichiometry, which is unsuitable for the formation of the desired template stoichiometry of 2 receptor:1 anion. This problem was overcome by the utilization of a cationic receptor containing an amide cleft anion recognition site as one of the ligands. As a consequence of favorable electrostatics and increased acidity of the amide and aryl protons, the pyridinium bisamide receptor $\mathbf{2}^+$ is designed to bind anions strongly in noncompetitive solvent media. Indeed, in acetone solution, ion-pairing between the pyridinium cation and the chloride anion in **2a** is very strong, as confirmed by ^{1}H NMR titration experiments with tetrabutylammonium (TBA) Cl^-, where an association constant of $>10^5$ M^{-1} was obtained for the equilibrium:[18]

$$TBA^+Cl^- + \mathbf{2d} \overset{K_{assoc}}{\rightleftharpoons} \mathbf{2a} + TBA^+PF_6^-$$

Complexation of the chloride anion occurs in the hydrogen bond donor cleft formed by the amide groups and their mutually *ortho*-aryl proton. The resulting tight ion-pair **2a** leaves the chloride anion with an unsaturated coordination sphere and presents an empty meridian available for binding another hydrogen bond donor ligand in the absence of a competitive solvent. As a preliminary test of this hypothesis, ^{1}H NMR titration of **1b** with **2a** in acetone-d_6 produced a 1:1 association constant of 100 M^{-1}, while an analogous titration experiment of **1b** with **2d** gave no evidence of association.

The macrocycle component was designed to act as the wheel through which an ion-pair, such as **2a**, would thread to form the [2]-pseudorotaxane. It was anticipated that an isophthalamide

(17) (a) Kavallieratos, K.; Bertao, C. M.; Crabtree, R. H. *J. Org. Chem.* **1999**, *64* (5), 1675−1683. (b) Kavallieratos, K.; de Gala, S. R.; Austin, D. J.; Crabtree, R. H. *J. Am. Chem. Soc.* **1997**, *119* (9), 2325−2326.
(18) It is also feasible to view this association constant as representative of the equilibrium:

$$Py^+ + Cl^- \overset{K_a}{\rightleftharpoons} \mathbf{2a}$$

Other possible equilibria in solution are:

$$TBA^+Cl^- \overset{K_1}{\rightleftharpoons} TBA^+ + Cl^-$$

$$\mathbf{2d} \overset{K_2}{\rightleftharpoons} Py^+ + PF_6^-$$

$$TBA^+ + PF_6^- \overset{K_3}{\rightleftharpoons} TBA^+PF_6^-$$

TBA salts are used frequently in anion-binding studies due to their noncompetitive nature; the dissociation constant, K_1, has been previously determined to be 16.6×10^4 M^{-1} in acetone: (a) Savedoff, L. G. *J. Am. Chem. Soc.* **1966**, *88* (4), 664−667. The PF_6^- anion is also commonly used in anion-binding studies due to its noncoordinating nature, that is, the dissociation constant, K_2, is very large, and the pyridinium countercation can be assumed to be "free" in solution (dissociation constant for $TBA^+PF_6^-$ ≈ 6300 M^{-1} in CH_2Cl_2): (b) Nelsen, S. F.; Ismagilov, R. F. *J. Phys. Chem. A* **1999**, *103*, 5373−5378. For ion-pairing with platinum complex cations, see: (c) Romeo, R.; Arena, G.; Scolaro, L. M.; Plutino, M. R. *Inorg. Chim. Acta* **1995**, *240*, 81−92.

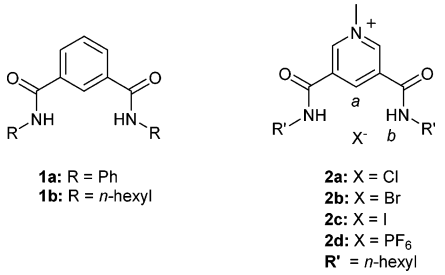

Figure 2. Structures of **1a**,**b** and **2a**−**d**.

anion recognition fragment incorporated within the macrocyclic cavity would satisfy the coordinatively unsaturated chloride anion. In addition, the integration of hydroquinone groups and polyether functionalities into the cyclic framework would stabilize the cationic pyridinium component of the ion-pair in the interpenetrated structure.

The new macrocycles, potential pyridinium, and pyridinium nicotinamide ion-pair threads (Figure 3) were prepared using standard organic synthetic procedures as described in the Supporting Information.

^{1}H NMR Binding Studies. The anion binding ability of macrocycles **3**−**5** was investigated initially by the addition of 1 molar equiv of anion, as its tetrabutylammonium (TBA) salt, to a solution of the macrocycle in acetone-d_6. Upon addition of Cl^-, Br^-, or I^-, there is an observed downfield shift in the macrocyclic amide and aryl protons (*e* and *d*), indicative of anion binding within the amide cleft. In addition, a downfield shift in the aromatic protons *h* is observed, whereas aromatic protons *i* remain unperturbed (see Figure 4). No perturbations in the ^{1}H NMR spectra of macrocycles **3**−**5** are observed upon addition of TBA hexafluorophosphate, indicative of an absence of anion binding.

Quantitative anion ^{1}H NMR titration experiments, in which the macrocycle amide (*e*), aryl (*d*), and hydroquinone (*h*) protons were monitored, gave a series of titration curves which were subsequently analyzed using the WinEQNMR[19] program, and determined association constants are presented in Table 1. This association constant is defined by the following equilibrium:

$$\text{macrocycle} + \text{TBA}\cdot\text{X}^- \overset{K_{a,exp}}{\rightleftharpoons} \text{macrocycle}\cdot\text{X}^- + \text{TBA}^+$$

Binding stoichiometries were confirmed by Job plot analyses. As expected, there is little difference in the anion binding

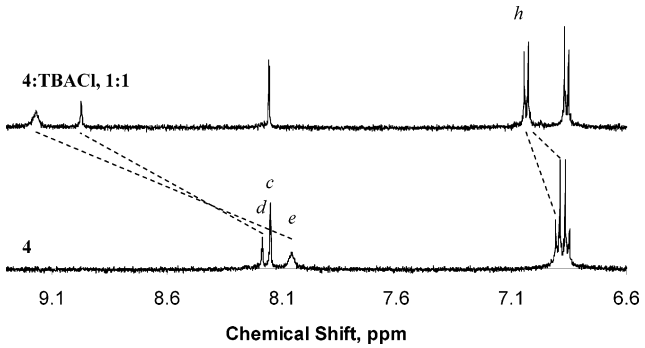

Figure 4. Observed perturbations in the aromatic region of the ^{1}H NMR of macrocycle **4** in acetone-d_6 at 293 K upon addition of 1 equiv of TBA chloride. Bottom: **4**. Top: **4** + TBACl.

Table 1. Association Constants, $K_{a,exp}$ (M^{-1}), for TBA Salts as Determined by ^{1}H NMR Titrations in Acetone-d_6 at 293 K (errors less than 10%)

anionic guest	3	4	5
Cl	2420	2560	2800
Br	480	470	685
I	45	50	60

affinities and selectivities between the three macrocycles. In all cases, chloride anions are the most strongly bound, followed by bromide and then iodide. This binding trend is a result of the near-identical nature of the isophthalamide anion binding cleft in the three systems. Chloride anions are bound most tightly as a result of increased hydrogen bond acceptor ability and through size match between the anion binding site and the ionic radius of the guest. Both bromide and iodide are larger anions as well as poorer hydrogen bond acceptors. No binding is observed for the large, noncoordinating hexafluorophosphate anion.

Initial evidence of pseudorotaxane formation came from the observed shifts in the ^{1}H NMR spectra of **2a** and macrocycle **4** in a 1:1 mixture in acetone-d_6 (Figure 5). A downfield shift in the macrocycle amide protons and aryl proton is indicative of anion complexation. In addition, upfield shifts of the amide protons of **2a** are postulated to be a result of polarization of the chloride anion toward the hydrogen bond donors of the macrocycle, which reduces the strength of hydrogen bonding between the pyridinium cation thread and the anion. Further evidence of the thread residing within the cavity is provided

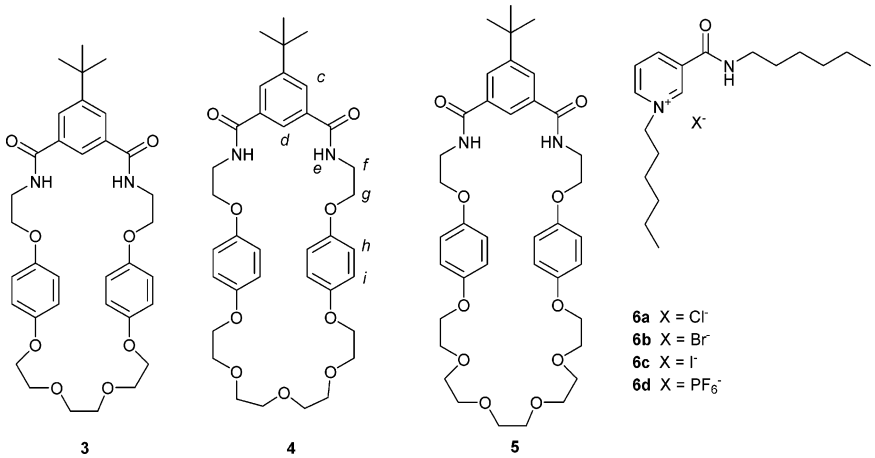

Figure 3. Structures of **3**−**5** and **6a**−**d**.

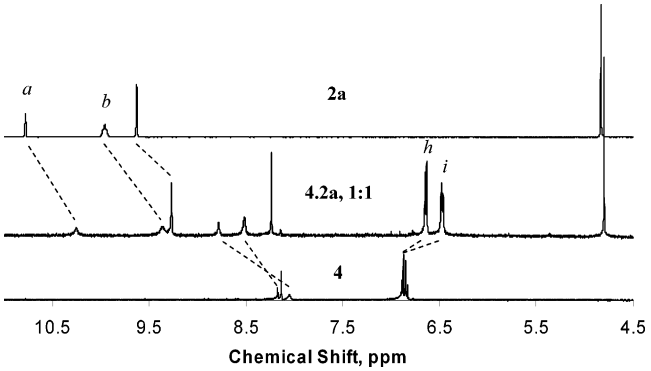

Figure 5. Observed perturbations in the aromatic region of the ^{1}H NMR of macrocycle **4** in acetone-d_6 at 293 K upon addition of 1 equiv of thread **2a**. Bottom: **4**. Middle: **4·2a**. Top: **2a**.

by significant upfield shifts in the macrocyclic hydroquinone protons and a shift in the pyridinium aryl proton, highly indicative of $\pi-\pi$ donor−acceptor stacking interactions.[20] It was observed that these ^{1}H NMR shift magnitudes were largest for **2a** and diminished in size, **2b** > **2c**. No shifts were observed in the 1:1 mixtures of the macrocycles with thread **2d**.

Analogous results were also obtained in the ^{1}H NMR spectra of a 1:1 mixture of the pyridinium nicotinamide thread **6a** and the macrocycles in deuterated acetone. Downfield shifts in the macrocycle amide and aryl proton indicate the binding of an anion within the cleft. Upfield shifts in the nicotinamide amide proton provide further evidence of threading, as polarization of the chloride anion toward the macrocycle perturbs the electronic environment. Upfield shifts in the macrocycle hydroquinone protons once more indicate the presence of $\pi-\pi$ donor−acceptor interactions in the complex and thus the thread residing within the cavity. As with the pyridinium threads, the magnitude of the observed shifts followed the trend $Cl^- > Br^- > I^-$, with no shifts being observed for **6d**, the hexafluorophosphate thread.

A quantitative ^{1}H NMR titration experiment for macrocycle **4** with pyridinium thread **2a** in acetone-d_6 at 293 K was carried out in which the macrocyclic amide, aryl, and hydroquinone protons were monitored and the data analyzed using the WinEQNMR[19] program. Initial assumptions led us to believe that this association constant, $K_{a,exp}$, was for the following equilibrium:

$$\text{thread}^+\cdot X^- + \text{macrocycle} \overset{K_{a,exp}}{\rightleftharpoons} \text{thread}^+X^-\cdot\text{macrocycle} \quad (1)$$

It is important, however, to consider other possible equilibria in solution, which could potentially be:

$$\text{thread}^+ + X^- \overset{K_1}{\rightleftharpoons} \text{thread}^+\cdot X^-$$

$$\text{macrocycle} + X^- \overset{K_2}{\rightleftharpoons} \text{macrocycle}\cdot X^-$$

$$\text{thread}^+ + \text{macrocycle} \overset{K_3}{\rightleftharpoons} \text{thread}^+\cdot\text{macrocycle}$$

The large association constant, K_1, for the pyridinium thread with a chloride counteranion indicates that the concentration of free anion in solution tends to zero. A binding constant of $>10^5$ M^{-1} was also obtained upon titration of TBA chloride with the pyridinium nicotinamide thread, **6d**, as would be expected considering the similarities between the two systems.[21] This would also limit the possible existence of a **4·Cl**$^-$ complex in solution, and hence K_2 will be virtually nonexistent. The lack of perturbations in the macrocyclic hydroquinone proton environment upon addition of pyridinium hexafluorophosphate thread, **2d**, indicates that K_3 is zero, which, again, is as expected due to the lack of a suitable templating anion. Conclusive proof for the ion-pair being the lone guest species in the pseudorotaxane assembly process comes from two important experimental observations. First, agreement between the association constants obtained by analysis of the macrocyclic amide protons, which are perturbed by the anion, and the macrocyclic hydroquinone protons, which undergo upfield perturbations as a result of the thread residing within the cavity, indicate that no free anion is complexed by the macrocycle.[22] Second, the association constants were found to be constant over a range of macrocycle concentrations (1.0, 1.5, 2.0, and 2.5×10^{-3} M). If the observed ^{1}H NMR shift was considered to be the weighted average of the two complexes, **4·Cl**$^-$ and **4·2a**, then the experimentally determined association constant can be considered to be representative of the two species and is expressed by one of the following two equations (K_{ipc}, defined by eq 1, represents the association constant for the ion-pair complex, e.g., **4·2a**):[23]

$$K_{a,exp} = \frac{K_1^{1/2}K_2}{[\mathbf{2a}]} + K_{ipc} \text{ for } K_2[\mathbf{4}] << 1$$

and

$$K_{a,exp} = \frac{(K_1K_2)^{1/2}}{([\mathbf{2a}][\mathbf{8}])^{1/2}} + K_{ipc} \text{ for } K_2[\mathbf{4}] >> 1$$

The first term in both equations represents the fraction of complex present in solution that is the macrocycle−anion complex, **4·Cl**$^-$, and the second is the fraction that is the ion-pair complex, **4·2a**. The invariance of the association constant with changing host and guest concentrations, therefore, indicates that no **4·Cl**$^-$ complex is formed, and thus the experimentally determined association constant is a true measure of the ion-pair association.

Quantitative ^{1}H NMR titration experiments were then carried out for all of the pyridinium-based threads, monitoring both the macrocyclic anion binding protons and the hydroquinone protons, and the obtained binding curves (Figure 6) were then analyzed using the WinEQNMR[19] program (Table 2). It is noteworthy that Table 2 shows pseudorotaxane formation is

(19) Hynes, M. J. *J. Chem. Soc., Dalton. Trans.* **1993**, 311−312.
(20) (a) Loeb, S. J.; Wisner, J. A. *Chem. Commun.* **2000**, 845−846. (b) Allwood, B. L.; Shahriari-Zavareh, H.; Stoddart, J. F.; Williams, D. J. *Chem. Commun.* **1987**, 1058−1061. (c) Kickham, J. E.; Loeb, S. J.; Murphy, S. L. *Chem.−Eur. J.* **1997**, *3* (8), 1203−1213.
(21) It is difficult to accurately determine such large binding constants; however, a linear plot was obtained for shift perturbations on additions of guest up to 1 equiv, at which point a plateau was observed and no perturbations seen upon further additions of TBA chloride.
(22) For titrations with **8** at initial concentrations of 1.0, 1.5, 2.0, and 2.5×10^{-3} M at 1 equiv of guest **2a** (from a 0.075 M solution) added, $\Delta\delta_{amide} = 0.42, 0.47, 0.51, 0.53$; $\Delta\delta_{aryl} = 0.54, 0.61, 0.67, 0.69$; and $\Delta\delta_{hydroquinone} = -0.32, -0.37, -0.40, -0.417$, respectively. Binding constants determined for **8** at initial concentrations of 1.5, 2.0, and 2.5×10^{-3} M are $K_{amide} = 2450$, 2460, and 2450 M^{-1}, and K_{aryl} and $K_{hydroquinone}$ determined values are in agreement within 10% experimental error.
(23) If macrocycle **8** also complexed **Cl**$^-$ in significant concentrations, then the determined association constants would be concentration-dependent, and a plot of $1/\{[\mathbf{2a}][\mathbf{8}]\}^{1/2}$ would give a straight line with an intercept equal to the true ion-pair complexation constant. For full mathematical treatment, see ref 15.

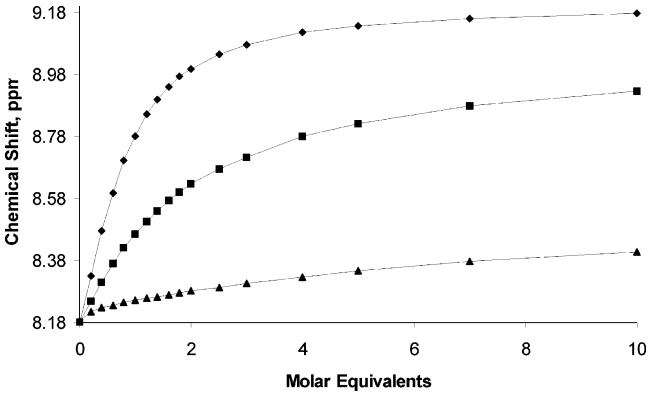

Figure 6. Example titration curves for threads **2a** (◆), **2b** (■), and **2c** (▲) with macrocycle **4** monitoring the *ortho*-aryl proton in acetone-d_6 at 293 K (initial host concentration, 1.5×10^{-3} M).

Table 2. Association Constants, $K_{a,exp}$ (M^{-1}), for Threads **2a**−**c** and **6a**−**c** as Determined by ^{1}H NMR Titrations in Acetone-d_6 at 293 K (errors less than 10%)

thread	3	4	5
2a	9500	2400	980
6a	1900	950	320
2b	610	700	120
6b	200	240	180
2c	<50[a]	65	<50[a]
6c	65	<50[a]	50

[a] Data could not be fitted using WinEQNMR due to very weak binding.

templated preferentially by the chloride anion pyridinium salts **2a** and **6a**, with no association being observed for the PF_6^- threads, **2d** and **6d**. This trend is a result of the complementary amide cleft size and geometry for chloride in preference to that of the larger halides, highlighting the essential role that the anion plays in the assembly process. In sharp contrast to the TBA anion salt-binding experiments, there is a large variation in binding strength across the macrocycles, with the smallest macrocycle, **3**, binding the pyridinium chloride threads, **2a** and **6a**, with a much greater affinity than for macrocycle **4** or **5**. The lowest association constants for chloride threading are observed for both systems with the largest macrocycle, **5**.

Possible reasons for the variation in association constants between macrocycles can be arrived at by considering the influence of the secondary interactions on the stability of the interpenetrated complex. It can be postulated that the smallest macrocycle maximizes both $\pi-\pi$ stacking and hydrogen bonding interactions with both pyridinium systems, and thus association is strong. The largest macrocycle, therefore, reduces the efficacy of both aromatic stacking and hydrogen bonding, primarily as a result of the polyether chain being too long and thus distorting the macrocycle geometry. In addition, the entropic loss on pseudorotaxane formation will be greatest for the larger macrocycle (vide infra). The smallest macrocycle could be said to possess the greatest size complementarity match with the pyridinium threads, which is also confirmed by the single-crystal X-ray structural evidence (vide infra).

While anion templation is still strong enough for pseudorotaxane formation, the pyridinium nicotinamide threads associate to a lesser extent with the macrocycles than do the pyridinium threads. A possible reason for this is the loss of stability provided by second-sphere pyridinium $N^+-CH_3\cdots$polyether hydrogen bonds (see Figure 7 and crystal structures in Figures 10 and 13). The trend across the range of macrocycles matches that observed for the pyridinium threads, which suggests that the size complementarity requirements of the nicotinamide threads do not differ significantly from those of the pyridinium analogues, especially in respect to the aromatic stacking interactions.

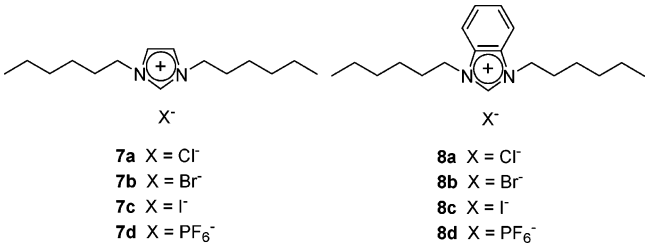

Figure 8. Structures of **7a**−**d** and **8a**−**d**.

Imidazolium, Benzimidazolium, and Guanidinium Pseudorotaxane Assemblies. Given the success of producing interpenetrated structures with pyridinium-based threading components, it was of interest to apply this anion templation principle further to include other potential cationic threads, such as imidazolium, benzimidazolium, and guanidinium. Imidazolium compounds have recently gained a great deal of attention due to many of their derivatives being room temperature ionic liquids (RTILs),[24] as well as readily accessible precursors to N-heterocyclic carbenes.[25] Furthermore, a variety of acyclic imidazolium derivatives have been shown recently to recognize anions,[26] with chloride and bromide anions exhibiting a templation role in the synthesis of bisimidazolium macrocycles.[27] Standard synthetic procedures were used to prepare the imidazolium and benzimidazolium salts (Figure 8).[28]

The guanidinium moiety is a well-established entity for anion binding, possessing both a positive charge and suitable hydrogen bond donors.[29] Potential guanidinium threads, **11a**−**d**, were prepared as shown in Scheme 1. Reaction of *n*-hexylisothiocyanate with *n*-hexylamine gave the thiourea, **9**, which was methylated using iodomethane to give the thiouronium iodide salt, **10**. Substitution with methylamine gave the guanidinium iodide salt, **11c**, which was converted to the chloride, bromide,

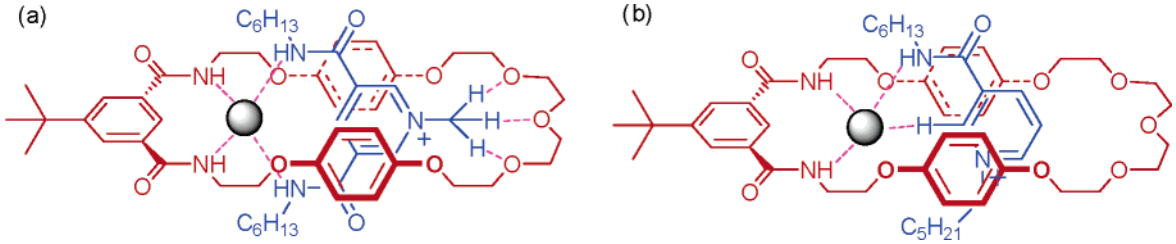

Figure 7. (a) Pyridinium-based pseudorotaxane assembly. (b) Pyridinium nicotinamide pseudorotaxane assembly (chloride anion represented by gray sphere).

Scheme 1

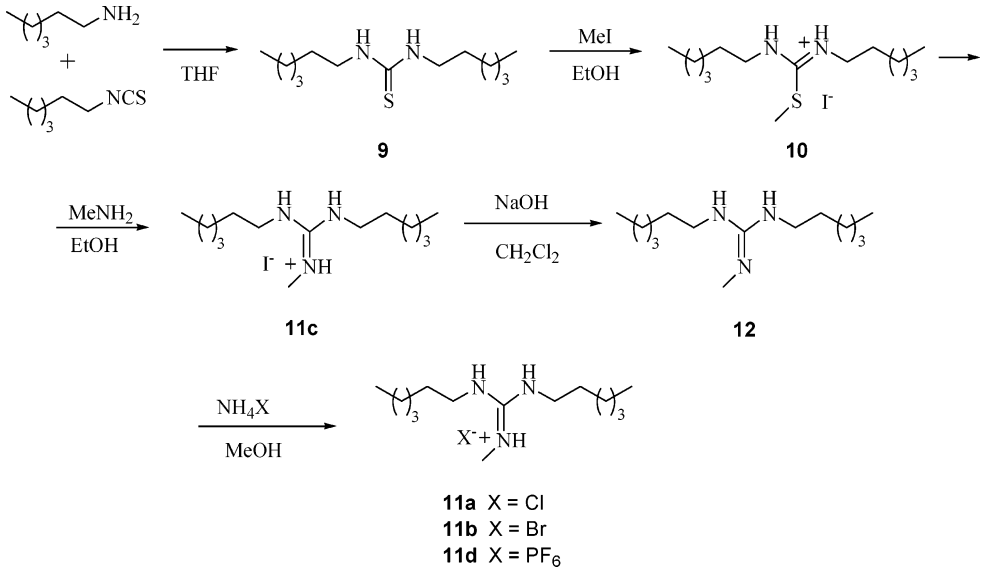

and hexafluorophosphate salts via the free guanidine base, **12**.

Initial evidence for threading of imidazolium and benzimidazolium pseudorotaxanes came from ^{1}H NMR spectra of 1:1 mixtures of threads **7a** and **8a** with macrocycle **4** in acetone-d_6. Downfield shifts in the macrocycle amide and *o*-aryl protons were observed along with upfield shifts in the CH proton in the 2-position of the ion-pair, indicative of the anion being bound within the amide cleft of the macrocycle. No perturbations of the ^{1}H NMR spectra were observed for **7d** and **8d**, with the magnitude of observed shifts for threads **a**−**c** following the trend $Cl^- > Br^- > I^-$. Larger upfield shifts in the macrocycle hydroquinone protons were observed for **7a** over **8a** (0.17 and 0.018 ppm, respectively), indicative of more significant $\pi-\pi$ stacking interactions. Despite the imidazolium threads having a positive charge density greater than that of the benzimidazolium analogues, the latter possess an increased aromatic surface area, and this is thought to be the reason for the increase in the role of $\pi-\pi$ stacking interactions in the final complex.

As with the previous pseudorotaxane systems, a ^{1}H NMR titration was initially carried out with thread **7a** and macrocycle **4** and an association constant, $K_{a,exp}$, determined as 1720 M^{-1} (acetone-d_6, 293 K). This association constant was found to be identical (within experimental error) for the binding curves obtained by monitoring the amide and anion binding aryl proton. It is unlikely, however, that these proton environments would differ significantly upon complexation with the free anion or the ion-pair, and thus they provide little information on the complexes present in solution.

The initial assumption was, again, that these $K_{a,exp}$ determinations were a direct measurement of the pseudorotaxane formation defined in eq 1. Interestingly though, the ion-pair association measured by titration of TBA chloride into a solution of known concentration of imidazolium hexafluorophosphate in acetone-d_6 at 293 K was determined to be 1800 M^{-1}. This value is significantly less than the ion-pairing strength of the pyridinium threads with chloride; it is also lower than the binding affinities displayed by the macrocycles for chloride anions. This led us to question whether the imidazolium cation will "follow" the anion into the macrocycle or simply compete for complexation of the anion with the macrocycle. As with the pyridinium systems, further equilibria and their association constants, K_1 to K_3, were also considered.

In this case, K_1, determined to be 1800 M^{-1}, indicates that some "free" anion may be present in solution, and hence association constant K_2 may be significant and contribute to the experimentally determined constant, $K_{a,exp}$. This relatively smaller magnitude of ion-pair association is likely, despite the strong electrostatic attraction between the two species, to stem from the presence of only one C−H···X^- hydrogen bond, in comparison to two amide NH···X^- and one CH···X^- hydrogen bond in the pyridinium ligands.

Investigation of the association constant determined by monitoring the shift perturbations of the macrocycle's hydroquinone protons, *h*, gave an association constant of 500 M^{-1} for macrocycle **4** titrated with the potential imidazolium chloride thread, **7a**. These shift perturbations must be a result of the ion-pair residing within the cavity, as the anion does not cause significant perturbations to this proton environment (as demonstrated with the TBA salt studies discussed previously) and the cationic thread itself cannot associate without a suitable anion, as shown by the lack of any proton shift changes with the imidazolium hexafluorophosphate ion-pair.[30]

(24) (a) Davis, J. J.; Fox, P. A. *Chem. Commun.* **2003**, 1209−1212. (b) Seddon, K. R. *J. Chem. Technol. Biotechnol.* **1997**, *68*, 351−356. (c) Branco, L. C.; Rosa, J. N.; Ramos, J. J. M.; Afonso, C. A. M. *Chem.—Eur J.* **2002**, *8* (16), 3671−3677. (d) Dzyuba, S. V.; Bartsch, R. A. *Chem. Commun.* **2001**, *16*, 1466−1467.
(25) (a) Arduengo, A. J.; Harlow, R. L.; Kline, M. *J. Am. Chem. Soc.* **1991**, *113* (1), 361−363. (b) Arduengo, A. J.; Rasika Dias, H. V.; Harlow, R. J.; Kline, M. *J. Am. Chem. Soc.* **1992**, *114* (14), 5530−5534. (c) Herrmann, W. A. *Angew. Chem., Int. Ed.* **2002**, *41*, 1290−1309.
(26) (a) Alcalde, E.; Alvarez-Rúa, C.; García-Granda, S.; García-Rodriguez, E.; Mequida, N.; Pérez-García, L. *Chem. Commun.* **1999**, 295−296. (b) Ihm, H.; Yun, S.; Kim, H. G.; Kim, J. K.; Kim, K. S. *Org. Lett.* **2002**, *4* (17), 2897−2900. (c) Sato, K.; Arai, S.; Yamagishi, T. *Tetrahedron Lett.* **1999**, *40* (28), 5219−5222.
(27) Alcalde, E.; Ramos, S.; Pérez-García, L. *Org. Lett.* **1999**, *1* (7), 1035−1038.
(28) Dzyuba, S. V.; Bartsch, R. A. *Chem. Commun.* **2001**, 1466−1467.
(29) (a) Best, M. D.; Tobey, S. L.; Anslyn, E. V. *Coord. Chem. Rev.* **2003**, *240*, 3−15. (b) Schmidtchen, F. P.; Berger, M. *Chem. Rev.* **1997**, *97*, 1609−1646.

Table 3. Experimentally Determined Association Constants, $K_{a,exp}$, and Ion-Pair Association Constants, K_{ipc} (eq 1), for Threads **7a**−**c** and **8a**−**c** as Determined by ^{1}H NMR Titrations in Acetone-d_6 at 293 K, with Initial Host Concentration at 1.5×10^{-3} M and Guest Feed Solution at 0.0375 M for Imidazolium and 0.01875 M for Benzimidazolium

	3		4		5	
thread	$K_{a,exp}$[a]	K_{ipc}[b]	$K_{a,exp}$[a]	K_{ipc}[b]	$K_{a,exp}$[a]	K_{ipc}[b]
7a	1340	400	1720	500	1690	230
8a	1630	320	2600	250	1200	200
7b	380	190	480	300	520	*c*
8b	390	240	500	230	370	110
7c	50	*c*	30	*c*	60	*c*
8c	40	80	30	90	50	*c*

[a] Estimated error = 10%. [b] Estimated error = 20%. [c] Shifts too small to determine binding constant; estimate less than 20 M^{-1}.

Further investigation of the **4·7a** complex formation in solution was achieved by titration of the ion-pair guest species into varying concentrations of the host molecule and the association constant determined. It was found that the association constants do vary with concentration, indicating the presence of both **4·7a** and **4·Cl**$^-$ complexes in solution. Significantly, however, the association constant determined by monitoring the hydroquinone protons involved in $\pi-\pi$ stacking interactions is invariant with concentration, within experimental error limits.

Typical values for $K_{a,exp}$ at macrocycle **4** concentrations of 1.5×10^{-3}, 1.75×10^{-3}, and 2.25×10^{-3} M are 1720, 1630, and 1500 M^{-1}, respectively, from monitoring the macrocycle aryl proton, *d*. A plot of $K_{a,exp}$ versus $1/\{[\mathbf{7a}][\mathbf{4}]\}^{1/2}$, or $1/\{[\mathbf{4}]\}^{1/2}$, gave a straight line, and the value of K_{ipc} was determined from the intercept to be 520 M^{-1}.[31] Importantly, the value of K_{ipc} determined via this method matches, within experimental error, the value determined via monitoring the macrocycle's hydroquinone protons, *h*. Table 3 gives the experimentally determined association constants from monitoring the amide and aryl protons to give $K_{a,exp}$, that is, the association constant representing the formation of both macrocycle·X^- and macrocycle·ion-pair complexes, and those determined by monitoring the hydroquinone protons to give K_{ipc}, that is, the association constant for pseudorotaxane formation.

Table 3 shows that the most strongly associated pseudorotaxanes are found with the chloride imidazolium and benzimidazolium salts, which mirrors the macrocycles' preference for this halide guest.[32] In contrast to the pyridinium systems, however, the magnitude of the chemical shift perturbations caused by $\pi-\pi$ stacking is significantly smaller, hence larger errors will be present due to the sensitivity limit of ^{1}H NMR. Large perturbations of the imidazolium methine proton are observed upon titration, indicating that the orientation of the imidazolium threads within the macrocycle is as shown in Figure 9.

Ion-pairing in the benzimidazolium chloride thread **8a** was measured by titration of TBA chloride into a solution of thread **8d** in acetone-d_6 at 293 K and determined to be 1800 M^{-1}. The

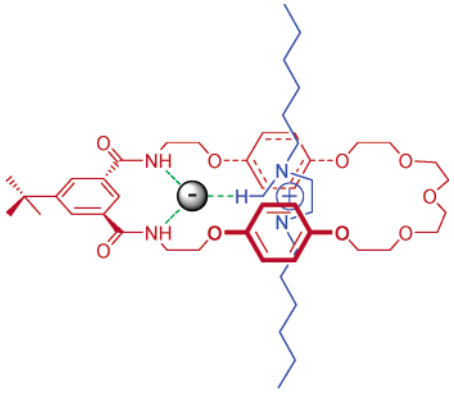

Figure 9. Proposed orientation of imidazolium thread **7a** within pseudorotaxane complex (chloride anion represented by gray sphere).

identical ion-pairing for the imidazolium and benzimidazolium is unsurprising considering the similarity in methine proton pK_a values reported for related *N*,*N*′-methyl derivatives: imidazolium = 23.0 and benzimidazolium = 21.6 in water at 25 °C.[33] Table 3 shows that relatively weaker pseudorotaxane complexes are formed with the benzimidazolium threads. This finding, coupled with similar $K_{a,exp}$ measurements, indicates that the macrocycle−anion complex is more predominant when the cationic thread is benzimidazolium. This must arise from either less effective secondary stabilizing interactions or from a greater entropic deficit on binding. It is notable, however, that the association constants for the benzimidazolium pseudorotaxanes can be determined with greater accuracy due to the larger magnitude of hydroquinone proton perturbations.

In contrast to the pyridinium chloride threads (Table 1), altering the macrocycle polyether ring size has a less dramatic affect on the association constant magnitudes of the imidazolium chloride guest species. Neither the imidazolium nor benzimidazolium threads possess the ability to hydrogen bond to the polyether chain in the same manner as the pyridinium salts, **2a**−**d**, due to a lack of suitable hydrogen bond donor functionality.[34]

A range of $K_{a,exp}$ values were determined for the guanidinium threads with macrocycles **3**−**5** in acetone-d_6 at 293 K. Macrocyclic amide and aryl protons were monitored, and in all cases, the determined values were considerably smaller in magnitude than those of all of the previous pseudorotaxane assemblies (Table 4). The strength of ion-pairing was again measured by titration of TBA chloride into a solution of the hexafluorophosphate salt, **11d**, in acetone-d_6 at 293 K. Monitoring the NH protons and analysis of the obtained titration curve gave a binding constant of 1500 M^{-1}. This is significantly less effective than the ion-pairing in the pyridinium systems and, like the imidazolium assemblies, implies that there will be a significant concentration of macrocycle−anion complex present in solution.

In all of the previous pseudorotaxane-assembled systems, evidence for the thread residing within the cavity was seen by significant upfield perturbations in the macrocyclic hydro-

(30) Due to the small shift perturbations in the hydroquinone protons caused by the imidazolium thread residing in the cavity, the errors for these association constants are estimated to be ±20% as a result of the sensitivity limit of ^{1}H NMR.
(31) Estimated errors on this value are ±30%.
(32) It is interesting to note the presence of an as-yet undetermined 1:2 host:guest binding contribution to the binding constants for the bromide and iodide threads, which is not present when the amide protons or the aryl proton is monitored. This contribution to the association is, although noticeable by Job plot analyses, very small in magnitude.
(33) Amyes, T. L.; Diver, S. T.; Richard, J. P.; Rivas, F. M.; Toth, K. *J. Am. Chem. Soc.* **2004**, *126* (13), 4366−4374.
(34) Attempts to further probe the imidazolium assembling motif by variable-temperature ^{1}H NMR proved fruitless, as even at −70 °C, the complexes and free species were found to still be in fast exchange. One noticeable feature, however, was the larger downfield shift observed in a mixture of **8:12a** (1.5×10^{-3}:3×10^{-3} M^{-1}) upon cooling, indicating that the nature of the complexation processes, as expected, is exothermic ($\Delta\delta_{amide}$ = 1.17, 1.21, 1.25, and 1.27 ppm at 20, 10, 0, and −10 °C, respectively).

Table 4. Experimentally Determined Association Constants, $K_{a,exp}$ (M^{-1}), for Threads **11a**−**c** as determined by ^{1}H NMR Titrations in Acetone-d_6 at 293 K (errors less than 10%)[a]

thread	**3**	**4**	**5**
11a	390	340	400
11b	310	320	370
11c	100	125	90

[a] $K_{a,exp}$ represents formation of both macrocycle−anion and macrocycle−ion-pair complexes.

Table 5. Isothermal Calorimetric Data for Complexes **2a·3** and **2a·4** Determined in 1,2-Dichloroethane at 298 K[a]

thread	macrocycle	*n*	K_a (M^{-1})	ΔH (cal mol^{-1})	ΔS (cal K^{-1})
2a	**3**	1	3.58×10^4	-1.186×10^4	−18.9
2a	**4**	1	3.06×10^5	-9.45×10^4	−295

[a] Errors < 10%.

quinone protons, and these perturbations could also be used to determine association constants. In the guanidinium systems, there is no electron-deficient aromatic surface within the thread, and hence no $\pi-\pi$ donor−acceptor interactions are present in the complex. Proof for the threading process was therefore obtained by undertaking intermolecular ^{1}H NMR NOE experiments. Saturation of the macrocyclic hydroquinone proton environment, *i*, resulted in a significant increase in the intensity of both guanidinium N^+−methyl and $NHCH_2$ protons. These guanidinium proton peak intensity perturbations arise from the proximity of the guanidinium thread residing within the cavity of the macrocycle.

The lack of $\pi-\pi$ donor−acceptor interactions in the pseudorotaxane complex results in an absence of secondary binding site with which to accurately measure the macrocycle−ion-pair association constant, K_{ipc}, and it becomes extremely difficult to accurately determine these values. Of significance though, is the small $K_{a,exp}$ values themselves, indicating that, although pseudorotaxane formation is occurring, it is a less effective assembling motif than the previously discussed pyridinium- and imidazolium-based systems.

Calorimetric Data. Isothermal calorimetry (ITC) allows the determination of ΔG^0, ΔH^0, and ΔS^0 for a ligand−receptor interaction by the measurement of stepwise changes in the enthalpy of interaction during the course of a single titration experiment.[35]

Binding constants for the pseudorotaxane systems in acetone were thought, from studying the ^{1}H NMR titration data, to be too low for ITC determination. A less competitive solvent system, 1,2-dichloroethane, was thus chosen and titrations were carried out (Table 5).

The association constants determined by this method, in agreement with the ^{1}H NMR titration data (Table 2), show a 1:1 stoichiometry for pseudorotaxane formation. As expected, the assembly process is enthalpically driven, with pseudorotaxane complex **2a·4** being more enthalpically favored. However, it is noteworthy that there is a greater entropic deficit upon binding for **2a·4**, −295 cal K^{-1}, in comparison to −18.9 cal K^{-1} for **2a·3**. Unfavorable entropic contributions in both systems arise from the loss of rotational and translational degrees of freedom upon pseudorotaxane association. Taking into account the conclusions drawn from the single-crystal X-ray diffraction evidence (vide infra), it is likely that increasing the length of the polyether chain results in a greater entropic deficit upon binding in order to maintain optimum anion recognition and $\pi-\pi$ stacking interactions.

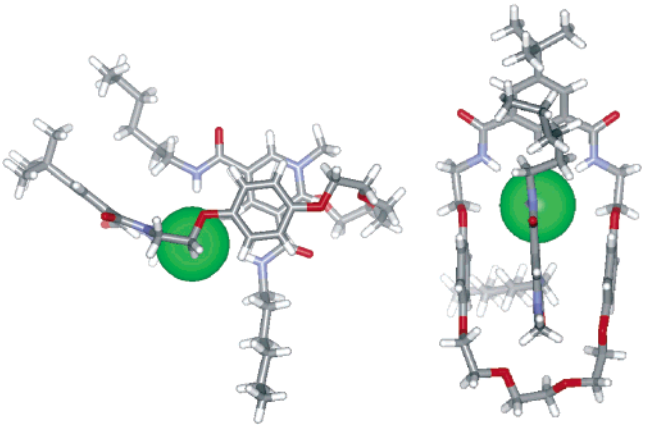

Figure 10. Solid-state structure of **2a·3**. Left: view in the plane of the macrocyclic ring. Right: view through the annulus of the macrocyclic ring. Chloride anion represented as CPK sphere for clarity.

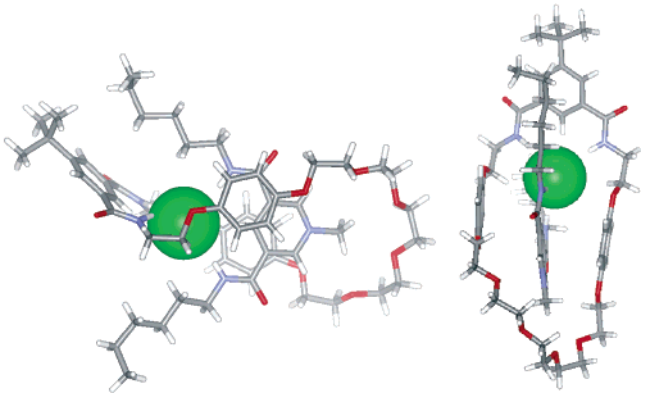

Figure 11. Solid-state structure of **2a·5**. Left: view in the plane of the macrocyclic ring. Right: view through the annulus of the macrocyclic ring. Chloride anion represented as CPK sphere for clarity.

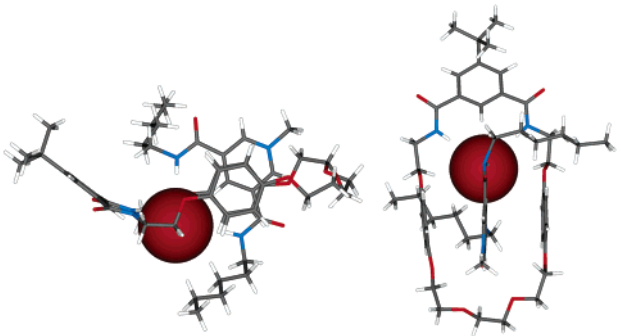

Figure 12. Solid-state structure of **2b·3**. Left: view in the plane of the macrocyclic ring. Right: view through the annulus of the macrocyclic ring. Bromide anion represented as CPK sphere for clarity.

Solid-State Evidence of Pseudorotaxane Formation. Further evidence of pseudorotaxane assembly comes from the solid state. Pale yellow crystals of macrocycle **7** with threads **2a**, **2b**,

(35) (a) Turnbull, W. B.; Daranas, A. H. *J. Am. Chem. Soc.* **2003**, *125* (48), 14859−14866. (b) Stulz, E.; Scott, S. M.; Bond, A. D.; Otto, S.; Sanders, J. K. M. *Inorg. Chem.* **2003**, *42*, 3086−3096. (c) Weber, P. C.; Salemme, F. R. *Curr. Opin. Struct. Biol.* **2003**, *13*, 115−121. (d) Leavitt, S.; Freire, E. *Curr. Opin. Struct. Biol.* **2001**, *11*, 560−566. (e) Rakharsky, M. V.; Inoue, Y. *Chem. Rev.* **1998**, *98*, 1875−1917. (f) Izatt, R. M.; Terry, R. E.; Haymore, B. L.; Hansen, L. D.; Dalley, N. K.; Avondet, A. G.; Christensen, J. J. *J. Am. Chem. Soc.* **1976**, *98*, 7620−7630.

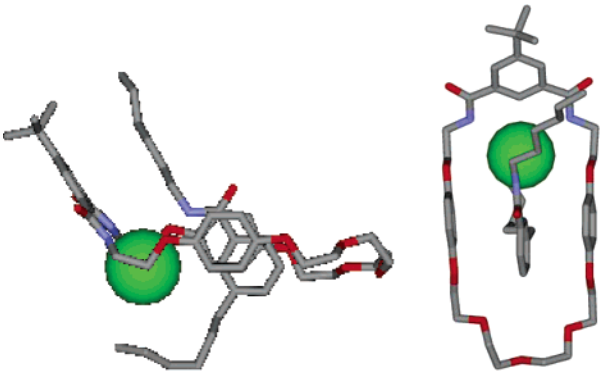

Figure 13. Solid-state structure of **12a·4**. Left: view in the plane of the macrocyclic ring. Right: view through the annulus of the macrocyclic ring. Chloride anion represented as CPK sphere and hydrogens omitted for clarity.

and **6a** and of macrocycle **5** with thread **2a** were grown by slow diffusion of diisopropyl ether into a 1:1 solution of the two components in acetone, chloroform, or 1,2-dichloromethane. ^{1}H NMR spectra of these crystals dissolved in acetone-d_6 are identical to that of a 1:1 mixture of the separate compounds. In all cases, single-crystal X-ray analysis reveals the ion-pair is threaded through the cavity of the macrocycle in the manner intended. In structure **2a·3** (Figure 10), the chloride anion is observed to have an octahedral geometry and engages in six hydrogen bonds with the hydrogen bond donor clefts of the macrocycle and the thread, as expected from solution evidence. Four short N−H···Cl$^-$ hydrogen bond contacts are observed, and NH···Cl distances are reported in Table 6. The pyridinium methyl group sits out of the plane of the polyether ring but still engages in N^+CH_3···O hydrogen bonding, with a typical distance of 3.370 Å. The hydroquinone rings are approximately parallel with respect to each other (within 6°) at a distance of ∼7 Å and sandwich the central pyridinium ring, indicative of aromatic stacking interactions.

The crystal structure of thread **2b** with the larger macrocycle, **5** (Figure 11), reveals that the chloride anion appears to possess distorted tetrahedral geometry and hydrogen bonds to the two molecular components through four short N−H···Cl contacts (Table 6). Hydrogen bonding between the pyridinium methyl group and the polyether chain is significantly shorter (2.987−3.175 Å) than in the previous structure as the methyl group appears to sit within the polyether chain. The hydroquinone groups interact with the pyridinium ring in the same manner as in **2a·3**, indicating that optimal aromatic stacking interactions are permitted despite the larger macrocycle size. This is likely to be due to the large flexibility inherent in the pentaethylene chain and results in a greater entropic loss upon complexation.

The structure of the bromide-templated pseudorotaxane complex, **2b·3** (Figure 12), shows the bromide anion possesses distorted trigonal bipyramidal geometry with the four N−H···Br$^-$ bonding distances being noticeably longer than those in the analogous chloride complex, **2a·3**. The methyl group again resides outside of the macrocycle, and observed hydrogen bonding is in the range of 3.383−3.446 Å.

The interpenetrated nature of the pyridinium nicotinamide threads with the macrocycle is demonstrated in the solid state by a structure of the chloride thread **6a** residing within the cavity of macrocycle **4** (Figure 13). In this system, only three N−H···Cl hydrogen bonds are possible; however, the chloride anion still retains an octahedral geometrical preference (Table 6). The nicotinamide ring is sandwiched between the two parallel hydroquinone units, and the lack of a suitable hydrogen donor in the correct position on the thread means that the polyether chain plays no role in further stabilization of the pseudorotaxane complex.

Table 6. Selected Crystallographic Data

complex	N–H···X	distance (Å)	angle (deg)	anion geometry
2a·3	N(1)···Cl(1)	3.383(3)	165.0(4)	octahedron
	N(2)···Cl(1)	3.396(3)	172.0(4)	
	N(4)···Cl(1)	3.386(4)	170.0(4)	
	N(5)···Cl(1)	3.359(3)	157.0(6)	
2a·5	N(1)···Cl(1)	3.349(2)	168.0(4)	distorted trigonal bipyramid
	N(2)···Cl(1)	3.376(2)	176.0(5)	
	N(4)···Cl(1)	3.400(2)	165.0(6)	
	N(5)···Cl(1)	3.303(2)	140.0(7)	
2b·3	N(1)···Br(1)	3.490(5)	171.0(2)	distorted tetrahedron
	N(2)···Br(1)	3.365(5)	160.0(2)	
	N(4)···Br(1)	3.424(6)	171.0(2)	
	N(5)···Br(1)	3.510(8)	173.0(2)	
12a·4	N(1)···Cl(1)	3.345(2)	169.0(2)	octahedron
	N(2)···Cl(1)	3.385(2)	164.0(2)	
	N(3)···Cl(1)	3.302(2)	169.0(3)	

Table 6 contains N−H···X$^-$ (X = Cl or Br) hydrogen bond lengths and the geometry of the templating anion within the pseudorotaxane complex for the four structures discussed.

Conclusions

A general anion templation procedure for assembling a wide range of pseudorotaxanes which contain positively charged pyridinium, pyridinium nicotinamide, imidazolium, benzimidazolium and guanidinium threading components, and macrocyclic isophthalamide polyether ligands has been developed. The templation strategy is based on coupling halide anion recognition with ion-pairing. In noncompetitive solvent media, a halide anion of a potential cationic threading component continues to be coordinatively unsaturated. Anion complexation by a macrocyclic ligand results in the interpenetration of the strongly associated cationic component of the ion-pair leading to a pseudorotaxane assembly. Extensive ^{1}H NMR titration investigations reveal that the thermodynamic stability of the pseudorotaxane assembly depends critically on the nature of the halide anion template, with chloride proving to be the optimum template anion, and also, importantly, on the strength of the ion-pairing between the anion template and the cationic thread. This ion-pair association strength is dictated by the character of the positively charged threading component. In the case of pyridinium-based systems, ion-pairing is extremely strong, whereas for imidazolium and guanidinium threads, weaker ion-pair association results in free anion−macrocycle complexation competing with pseudorotaxane formation. In addition, the efficacy of favorable second-sphere $\pi-\pi$ aromatic stacking interactions between the positively charged pyridinium threading component and the hydroquinone units of the respective macrocyclic ligand, together with favorable second-sphere pyridinium N^+-CH_3···polyether macrocycle hydrogen bonding interactions, is dictated by macrocyclic polyether ring size. In contrast, imidazolium and guanidinium pseudorotaxane stability is not affected significantly by macrocycle ring size. Preliminary isothermal calorimetric studies indicate, as expected, that pseudorotaxane assembly is an enthalpically driven process, opposed by entropy. Single-crystal X-ray structural determina-

tions reveal solid-state evidence of pseudorotaxane formation, highlighting the role of anion recognition, aromatic $\pi-\pi$ stacking, and hydrogen bonding interactions in the stabilization of the interpenetrated supramolecular assembly. Efforts are currently being made to exploit this anion templation strategy to produce related rotaxane[36] and catenane[37] derivatives for anion sensing and molecular machinelike behavior.[38]

Experimental Section

General Methods. Chemicals were purchased from Aldrich and used as received with the exception of thionyl chloride which was distilled prior to use according to standard laboratory procedures. Deionized water was used in all cases. All reactions were carried out under an atmosphere of dry nitrogen, unless otherwise stated. ^{1}H and ^{13}C NMR were recorded on Varian 300 MHz Mercury VX Works and 500 MHz Unity Plus spectrometers. Mass spectrometry was carried out using a Micromass LCT electrospray mass spectrometer. Elemental analyses were performed by the Inorganic Chemistry Laboratory Microanalysis service. All melting point determinations are uncorrected.

***N,N′*-Di(1-hexyl)thiourea (15).** To a solution of *n*-hexyl isothiocyanate (2.86 g, 20 mmol) in THF (50 mL) was added *n*-hexylamine (2.23 g, 22 mmol), and the reaction mixture was stirred under reflux for 3 h. The volume of the mixture was reduced (10 mL), and hexane (50 mL) was added. Finally, the solution was concentrated to 35 mL, and the product crystallized at −20 °C overnight. The white crystalline product was separated, washed with cold hexane, and dried in vacuo to give the title compound in 94% yield (4.6 g) as white powder. Mp 34−38 °C. ^{1}H NMR (300 MHz, $CDCl_3$, TMS): δ 5.80 (br s, 2H, $CH_2CH_2NHC{=}S$), 3.38 (br s, 4H, $CH_2CH_2NHC{=}S$), 1.58 (qi, $J = 6.1$ Hz, 4H, $CH_2CH_2NHC{=}S$), 1.38−1.27 (m, 12H, $CH_3(CH_2)_3CH_2CH_2NH$), 0.87 (t, $J = 6.7$ Hz, 6H, CH_3CH_2). ^{13}C NMR ($CDCl_3$): δ 181.4, 44.4, 31.4, 29.0, 26.6, 22.5, 14.0. FI MS $[C_{13}H_{28}N_2S]^+$: *m*/*z* observed 244.1975 (100), calcd 244.1973. Elemental analysis calcd for $C_{13}H_{28}N_2S$: C, 63.88; H, 11.55; N, 11.46. Found: C, 64.04; H, 11.64; N, 11.66.

***N,N′*-Di(1-hexyl)-(*S*)-methylisothiouronium Iodide (16).** To a solution of thiourea (**15**) (4.15 g, 17 mmol) in ethanol (40 mL) was added iodomethane (4.82 g, 34 mmol), and the mixture was stirred at 40−45 °C for 4 h and at 70 °C for 1 h. Evaporation of the solvent and drying of the oily residue in vacuo gave the title compound in 98% yield as colorless oil (6.4 g). ^{1}H NMR (300 MHz, $CDCl_3$, TMS): δ 8.55 and 7.94 (2 × br s, 2H, $CH_2CH_2N^+H{=}C(SCH_3)NHCH_2CH_2$), 3.76 and 3.46 (2 × br s, 4H, $CH_2CH_2N^+H{=}C(SCH_3)NHCH_2CH_2$), 2.86 (s, 3H, SCH_3), 1.71 (br s, 4H, CH_2CH_2NH), 1.36−1.26 (m, 12H, $CH_3(CH_2)_3CH_2CH_2NH$), 0.84 (t, $J = 6.0$ Hz, 6H, CH_3CH_2). ^{13}C NMR (300 MHz, $CDCl_3$, TMS): δ 45.3, 31.3, 29.4, 26.4, 22.5, 16.3, 14.1. ESI MS $[C_{14}H_{31}N_2S - I]^+$: *m*/*z* observed 259.2199, calcd 259.2208. Elemental analysis calcd for $C_{14}H_{31}IN_2S$: C, 43.52; H, 8.09; N, 7.25. Found: C, 44.17; H, 8.09; N, 7.43.

***N,N′*-Di(1-hexyl)-*N″*-methylguanidine Hydrochloride (17a).** To a solution of guanidine (**18**) (0.6 g, 2.5 mmol) in methanol (20 mL) was added NH_4Cl (0.14 g, 2.5 mmol), and the solution was refluxed for 2 h. Evaporation of solvent resulted in an oily residue which was dried in vacuo to give the title compound in quantitative yield as colorless solid (0.69 g). ^{1}H NMR (300 MHz, $CDCl_3$, TMS): δ 7.80 (q, $J = 4.7$ Hz, 1H, $=N^+HCH_3$), 6.95 (t, $J = 5.3$ Hz, 2H, CH_2CH_2NHC), 3.41 (q, $J = 5.8$ Hz, 4H, CH_2CH_2NHC), 3.02 (d, $J = 4.8$ Hz, 3H, $=N^+HCH_3$), 1.65 (qi, $J = 7.2$ Hz, CH_2CH_2NHC), 1.39−1.26 (m, 12H, $CH_3(CH_2)_3CH_2CH_2NHC$), 0.88 (t, $J = 6.6$ Hz, 6H, CH_2CH_3). ^{13}C NMR (300 MHz, $CDCl_3$, TMS): δ 155.7, 42.5, 31.4, 29.1, 29.0, 26.4, 22.5, 14.0. ESI MS $[C_{14}H_{32}N_3 - Cl]^+$: *m*/*z* observed 242.2598, calcd 242.2596. Elemental analysis calcd for $C_{14}H_{32}ClN_3$: C, 60.51; H, 11.61; N, 15.12. Found: C, 59.34; H, 11.86; N, 15.31.

***N,N′*-Di(1-hexyl)-*N″*-methylguanidine Hydrobromide (17b).** To a solution of guanidine (**18**) (0.6 g, 2.5 mmol) in methanol (20 mL) was added NH_4Br (0.24 g, 2.5 mmol), and the solution was refluxed for 2 h. Evaporation of solvent resulted in an oily residue which was dried in vacuo to give the title compound in quantitative yield as pale-yellow waxy material (0.81 g). ^{1}H NMR (300 MHz, $CDCl_3$, TMS): δ 7.28 (q, $J = 4.8$ Hz, 1H, $=N^+HCH_3$), 6.54 (t, $J = 5.1$ Hz, 2H, CH_2CH_2NHC), 3.36 (q, $J = 6.0$ Hz, 4H, CH_2CH_2NHC), 2.98 (d, $J = 4.8$ Hz, 3H, $=N^+HCH_3$), 1.59 (qi, $J = 7.2$ Hz, CH_2CH_2NHC), 1.36−1.24 (m, 12H, $CH_3(CH_2)_3CH_2CH_2NHC$), 0.88 (t, $J = 6.6$ Hz, 6H, CH_2CH_3). ^{13}C NMR (300 MHz, $CDCl_3$, TMS): δ 155.5, 42.3, 31.3, 29.1, 29.0, 26.4, 22.5, 14.0. ESI MS $[C_{14}H_{32}N_3 - Br]^+$: *m*/*z* observed 242.2596 (100), calcd 242.2596. Elemental analysis calcd for $C_{14}H_{32}BrN_3$: C, 52.17; H, 10.01; N, 13.04. Found: C, 52.12; H, 10.17; N, 12.80.

***N,N′*-Di(1-hexyl)-*N″*-methylguanidine Hydroiodide (17c).** A solution of (*S*)-methyl derivative (**16**) (6.3 g, 16.3 mmol) in ethanol (40 mL) containing methylamine (6.5 g, 210 mmol) was stirred at 42−45 °C for 3 h and at 70 °C for 2 h. After evaporation of the volatile parts, the oily residue was dried in vacuo to give the title compound in quantitative yield as colorless viscous oil (6 g). ^{1}H NMR (300 MHz, $CDCl_3$, TMS): δ 6.91 (q, $J = 4.9$ Hz, 1H, $=N^+HCH_3$), 6.23 (t, $J = 5.4$ Hz, 2H, CH_2CH_2NHC), 3.43 (q, $J = 6.6$ Hz, 4H, CH_2CH_2NHC), 3.05 (d, $J = 4.6$ Hz, 3H, $=N^+HCH_3$), 1.66 (qi, $J = 7.6$ Hz, CH_2CH_2NHC), 1.36−1.26 (m, 12H, $CH_3(CH_2)_3CH_2CH_2NHC$), 0.86 (t, $J = 6.8$ Hz, 6H, CH_2CH_3). ^{13}C NMR (300 MHz, $CDCl_3$, TMS): δ 154.7, 42.7, 31.4, 29.3, 29.0, 26.3, 22.5, 14.0. ESI MS $[C_{14}H_{32}N_3 - I]^+$: *m*/*z* observed 242.2587, calcd 242.2596. Elemental analysis calcd for $C_{14}H_{32}IN_3$: C, 45.53; H, 8.73; N, 11.38. Found: C, 46.06; H, 8.64; N, 11.51.

***N,N′*-Di(1-hexyl)-*N″*-methylguanidine Hexafluorophosphate (17d).** Obtained from guanidine (**18**) (0.48 g, 2 mmol) and NH_4PF_6 (0.33 g, 2 mmol), employing the above procedure, **17d** resulted in quantitative yield as pale yellow oil (0.77 g). ^{1}H NMR (300 MHz, $CDCl_3$, TMS): δ 5.66 (q, $J = 5.0$ Hz, 1H, $=N^+HCH_3$), 5.29 (t, $J = 5.3$ Hz, 2H, CH_2CH_2NHC), 3.22 (q, $J = 5.6$ Hz, 4H, CH_2CH_2NHC), 3.93 (d, $J = 4.8$ Hz, 3H, $=N^+HCH_3$), 1.65 (qi, $J = 6.5$ Hz, CH_2CH_2NHC), 1.40−1.28 (m, 12H, $CH_3(CH_2)_3CH_2CH_2NHC$), 0.89 (t, $J = 6.6$ Hz, 6H, CH_2CH_3). ^{13}C NMR (300 MHz, $CDCl_3$, TMS): δ 155.0, 41.8, 31.2, 28.4, 27.8, 26.1, 22.4, 13.9. ESI MS $[C_{14}H_{32}N_3 - PF_6]^+$: *m*/*z* observed 242.2586 (100), calcd for $C_{14}H_{32}N_3^+$ $(M - PF_6)^+$ 242.2596. Elemental analysis calcd for $C_{14}H_{32}F_6N_3P$: C, 43.41; H, 8.33; N, 10.85. Found: C, 44.06; H, 9.04; N, 11.02.

***N,N′*-Di(1-hexyl)-*N″*-methylguanidine (18).** A solution of guanidine hydroiodide (**17c**) (0.96 g, 2.6 mmol) in CH_2Cl_2 (35 mL) was vigorously stirred with 6 M sodium hydroxide solution (6 mL) for 30 min. The organic layer was separated, dried over K_2CO_3, evaporated, and the residue dried in vacuo to give the free base in quantitative yield as colorless viscous oil (0.63 g). ^{1}H NMR (300 MHz, DMSO-d_6, TMS): δ 4.82 (br s, 2H, CH_2CH_2NHC), 2.87 (t, $J = 6.8$ Hz, 4H, CH_2CH_2NHC), 2.53 (s, 3H, $=NCH_3$), 1.42−1.26 (m, 16H, $CH_3(CH_2)_4CH_2NHC$), 0.84 (t, $J = 6.3$ Hz, 6H, CH_2CH_3). ^{13}C NMR (300 MHz, DMSO-d_6, TMS): δ 152.9, 43.0, 31.7, 30.8, 30.3, 26.9, 22.6, 14.4. ESI MS $[C_{14}H_{31}N_3 + H]^+$: *m*/*z* observed 242.258, calcd 242.2596.

Typical ^{1}H NMR Titration Procedure. All titrations were performed with the starting concentration of hosts **7**, **8**, and **9** at 1.5×10^{-3} M and the addition of appropriate aliquots of titrant (0.2, 0.4−1.8, 2.0, 2.5, 3.0, 4.0, 5.0, 7.0, and 10.0 equiv) to the NMR sample with a 10, 25, or 50 μl microsyringe as appropriate. The macrocycle aryl proton *d* was followed during the course of the titration, and the data were fitted and analyzed to give association constants using the WinEQNMR program.[21] Following the macrocycle amide protons *e* gave association constants in agreement within experimental error. Unless stated otherwise, all titration curves fit 1:1 binding models and estimated errors were less than 10%.

(36) Wisner, J. A.; Beer, P. D.; Drew, M. G. B.; Sambrook, M. R. *J. Am. Chem. Soc.* **2002**, *124* (42), 12469−12476.
(37) Sambrook, M. R.; Beer, P. D.; Wisner, J. A.; Paul, R. L.; Cowley, A. *J. Am. Chem. Soc.* **2004**, *126*, 15364−15365.
(38) Keaveney, C. M.; Leigh, D. A. *Angew Chem., Int. Ed.* **2004**, *43* (10), 1222−1224.

Calorimetry. All binding experiments were performed in anhydrous 1,2-dichloroethane purchased from Aldrich and stored over activated 3 Å molecular sieves. The solvent was ultrasonically degassed under vacuum before use. All binding experiments were performed on a VP−ITC Isothermal Calorimeter from Microcal Inc. (Northampton, MA), with a stirring rate of 300 rpm, a constant temperature of 25 °C, and 50−70 injections of 3−5 μL per injection. Experiments were run with cell concentrations of the macrocycle in the range of 0.05−5 mmol and ion-pair concentrations in the titration syringe at 10 times the concentration used in the cell. The range used was necessary to generate data over a wide range of K_a values observed that would give acceptable curve fitting during data analysis. Dilution effects for all titrations were determined by a second experiment adding the same ion-pair solution into a pure 1,2-dichloroethane solution and subtracting the result from the raw titration to produce the final binding curve. Association constants and thermodynamic parameters were obtained in all cases by fitting the final binding curve using a one-site model in the Origin 7 software supplied with the instrument. Curves were fitted by variation of all three experimentally determined parameters (n, K_a, ΔH) and gave excellent agreement to the data for all titrations. Note that in all curves, the first three data points were removed due to systematic errors generated by loading of the syringe into the cell.

X-ray Crystallography. Crystal data for **2a·3**·0.8H_2O: M = 1005.06, monoclinic, space group $P121/c1$, a = 10.871(2), b = 15.8369(2), c = 33.7208(3), α = 90, β = 90.7775(3), γ = 90°, U = 5808.73(14) Å^3, Z = 4, R = 0.1344, wR = 0.1022. Crystal data for **2a·5**: M = 1078.79, monoclinic, space group $P121/n1$, a = 16.0174, b = 10.3218(1), c = 35.6876(3), α = 90, β = 100.8331(4), γ = 90°, U = 795.03(8) Å^3, Z = 4, R = 0.0425, wR = 0.0471. Crystal data for **2b·3**: M = 1035.13, monoclinic, space group $P121/c1$, a = 10.88110(10), b = 16.0952(2), c = 33.5237(4), α = 90, β = 90.6073(4), γ = 90°, U = 5870.79(11) Å^3, Z = 4, R = 0.1071, wR = 0.1404. Crystal data for **12a·4**: M = 977.68, monoclinic, space group $P121/n1$, a = 11.03740-(10), b = 21.5071(3), c = 22.7595(3), α = 90, β = 100.9476(5), γ = 90°, U = 5304.38(11) Å^3, Z = 4, R = 0.0426, wR = 0.0551. Single crystals of **2a·3**, **2b·3**, **2a·5**, and **12a·4** were coated with perfluoropolyether oil, mounted on a glass fiber, and cooled rapidly to 150 K in a stream of cold N_2 using an Oxford Cryosystems CRYOSTREAM unit. Diffraction data were measured using an Enraf-Nonius KappaCCD diffractometer (graphite monochromated Mo Kα radiation, λ = 0.71073 Å). Intensity data were processed using the DENZO−SMN package.[39] The structure was solved by direct methods using the SIR92 program.[40] Full-matrix least-squares refinement was carried out using the CRYSTALS program suite.[41] The N−H atoms were located in the difference Fourier maps and the coordinates and isotropic thermal parameters subsequently refined. All other hydrogen atoms were positioned geometrically after each cycle of refinement. A Chebychev polynomial weighting scheme was applied. In compounds **2b·3** and **12a·4**, disorder was encountered in the hexyl chains of the thread. The disorder was modeled appropriately. Crystallographic data for the compounds are listed in the Supporting Information.

Acknowledgment. We thank EPSRC for postdoctoral fellowships (J.A.W. and F.S.) and a studentship (M.R.S.). Financial support for Dr. Wisner from the Natural Sciences and Engineering Research Council of Canada is also acknowledged.

Supporting Information Available: Synthetic procedures and characterization data for threads **2a**−**d**, macrocycles **3**−**5**, and threads **6a**−**d**. Tables giving the crystal data and structure refinement information, bond lengths and bond angles, atomic and hydrogen coordinates, and isotropic and anisotropic displacement coordinates for structures **2a·7**, **2a·9**, **2a·7**, and **12a·8**. Figure demonstrating the ^{1}H NMR intermolecular NOE experiment carried out for complex **17a·8**. This material is available free of charge via the Internet at http://pubs.acs.org.

JA046278Z

(39) Otwinowski, Z.; Minor, W. Processing of X-ray Diffraction Data Collected in Oscillation Mode. *Methods Enzymol.* **1997**, 276.
(40) Alotmare, A.; Cascarano, G.; Giacovazzo, G.; Guagliardi, A.; Burla, M. C.; Polidori, G.; Camalli, M. *J. Appl. Crystallogr.* **1994**, *27* (3), 435−435.
(41) Watkin, D. J.; Prout, C. K.; Carruthers, J. R.; Betteridge, P. W.; Cooper, R. I. *CRYSTALS*, issue 11; Chemical Crystallography Laboratory: Oxford, U.K., 2001.